Automatic Generation of Head Models for EEG Source Analysis from MRI

Benjamin Lanfer[12], Isabella Paul-Jordanov[1], Michael Scherg[1], Carsten H. Wolters[2]

1 BESA GmbH, Gräfelfing, Germany

2 Institut für Biomagnetismus und Biosignalanalyse, Westfälische Wilhelms-Universität Münster, Germany

I INTRODUCTION

EEG source analysis greatly benefits from using individual, realistically shaped head models for the solution of the forward problem [1,2]. Routine application of individual head models is still impeded by the difficulty of correctly segmenting MRI data, especially bone and cerebrospinal fluid (CSF). For this reason, we propose a new, automated segmentation procedure on the basis of T1- and T2-weighted MR images. The good performance of this approach is demonstrated by exemplary segmentation results and validation against a CT reference segmentation.

II MATERIALS and METHODS

The Segmentation Approach

- ➢ Bayesian segmentation approach incorporating a Markov Random Field (MRF) model of the anatomy of the human head.
- ➢ MRF model represents layered structure of eight different head tissues.
- ➢ Definition of MRF through Gibbs Random Field:

Bayes' formula

$$P(x \mid \boldsymbol{y}) = \underbrace{l(\boldsymbol{y} \mid x, \boldsymbol{\lambda})}_{\text{Likelihood}} \cdot \underbrace{P(x)}_{\text{Prior}}$$

$$P(x) \propto \exp\left(-\frac{1}{T} \underbrace{\sum_{i \in \mathcal{S}} \left\{ V_1(x_i, i) + \sum_{i' \in \mathcal{N}_i} V_2(x_i, x_{i'}, i, i') \right\}}_{\text{Gibbs energy } U(x)} \right)$$

$$\underbrace{V_2(x_i, x_{i'}, i, i')}_{\text{Pairwise clique potentials}} = -\ln \underbrace{P_{x_i, x_{i'}}(i, i')}_{\text{Pseudo transition probabilities}}$$

- ➢ Pseudo transition probabilities are defined according to connectivity graphs (Fig. 2).
- ➢ Relative positions of neighbouring voxels to reference surfaces (white matter, scalp) are taken into account.
- ➢ Optimization procedure based on the Expectation-Maximization (E-M) [3] algorithm (Alg. 1).

The CT Validation Study

- ➢ CT as reference modality - good contrast between skull bone and soft tissues.
- ➢ Compare skull segmentation results from proposed approach, T, to CT based reference segmentation, R, using Dice coefficient:

$$D(R,T) = \frac{2\,|R \cap T|}{|R| + |T|}$$

- ➢ Coregistration of MRIs to CT image using pre-segmented scalp masks and ROI.
- ➢ Construction of CT based reference skull segmentation (Fig. 4) by thresholding and additional manual cleaning up. Air cavities are labeled as skull.

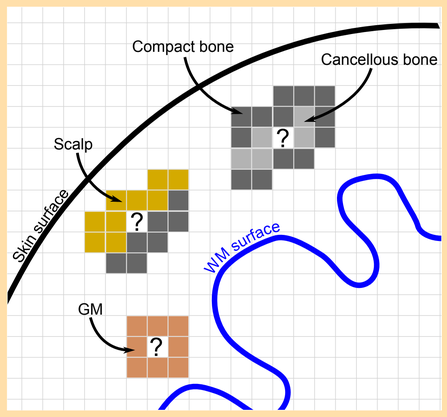

Fig. 1
Illustration of the segmentation approach's principal idea.

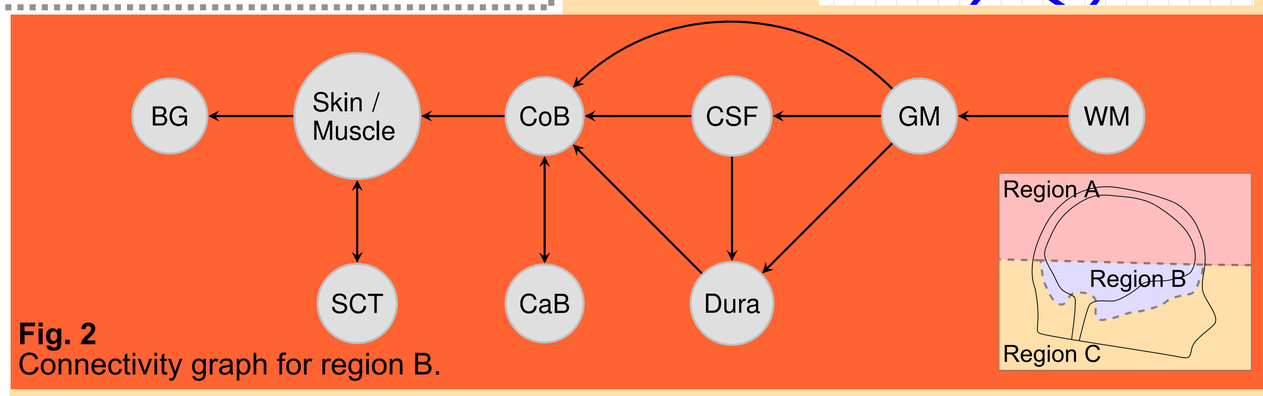

Fig. 2
Connectivity graph for region B.

Alg. 1
The proposed segmentation algorithm.

Require: $\boldsymbol{y}$ (image data), t^{max} (max. number of iterations), $M^{\text{ref. scalp}}$, M^{WM} (scalp and WM reference surfaces)

1: Preprocessing
2: Initial guess for segmentation x and gray value parameters $\boldsymbol{\lambda}$
3: $t \leftarrow 0$
4: **repeat**
5: E-step: $x_i^{(t+1)} = \arg\max_c P(X_i = c \mid \boldsymbol{y}_i, \boldsymbol{\lambda}^{(t)}, x_{\mathcal{N}_i}),\ \forall i \in \mathcal{S}$ (Iterated Conditional Modes (ICM) [5]).
6: M-step: Compute $\boldsymbol{\lambda}^{(t+1)}$
7: $t \leftarrow t + 1$
8: **until** $(x_i^{(t)} = x_i^{(t-1)}, \forall i \in \mathcal{S}) \ \vee \ (t \geq t^{\text{max}})$
9: Postprocessing

III RESULTS

Exemplary Results

- ➢ Scalp, skull, CSF, and brain outlines of exemplary segmentations based on a T1- and a T2-MRI (Fig. 3a), resp., based only on a T1-MRI (Fig. 3b).
- ➢ Accurate skull segmentation. Only minor inaccuracies where the inner scalp / muscle layer is misclassified due to low SNR or water-fat shift artifact. Suitable for construction of EEG head models [4].
- ➢ Good accuracy also for other tissues. Most notably also good CSF segmentation even when only T1-MRI data is available.
- ➢ Segmentation results can directly be used as a basis for constructing geometry-adapted hexahedral FE meshes for the solution of the EEG forward problem.

Validation vs. CT Reference Segmentation

- ➢ Dice coefficients for reference skull mask and ...
  ... segmentation based on T1- and T2-weighted image: $D = 0.863$
  ... segmentation based on T1-weighted image only: $D = 0.843$
- ➢ Our proposed method compares favorably with previously published methods for skull segmentation (e.g., [6]). In their very similar CT validation study Wang et al. measured a Dice coefficient of 0.75 for their proposed approach, and a coefficient of 0.70 for the approach from [7].

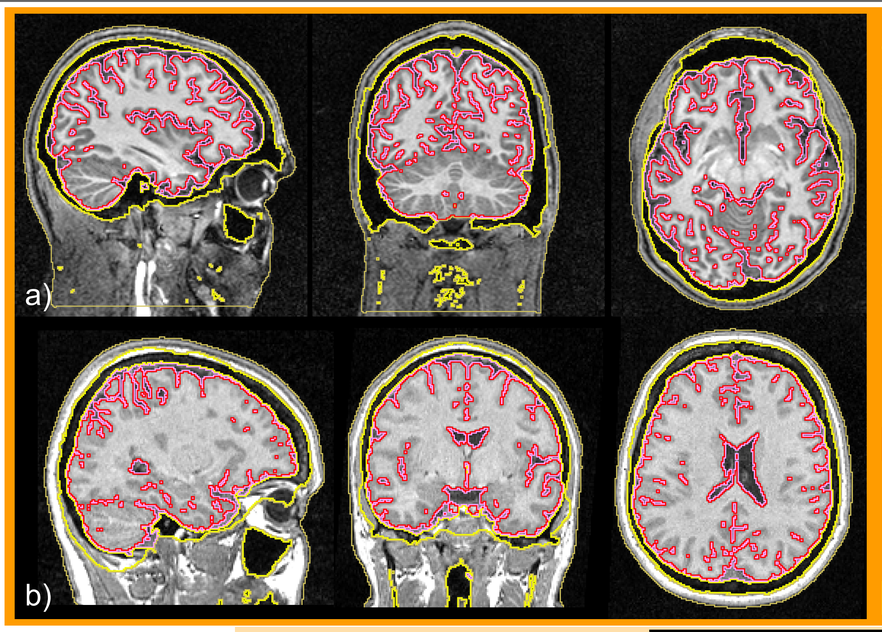

Fig. 3
Tissue outlines of segmentation results based on a) T1- and T2-MRI, and b) on T1-MRI only overlaid onto orthogonal slices of T1-MRI. Results were relabeled from eight to four tissues (see legend) for a clearer presentation.

- Scalp (muscle/scalp and subcutaneous tissue)
- Skull (compact and cancellous bone)
- CSF (CSF and dura mater)
- Brain (GM and WM)

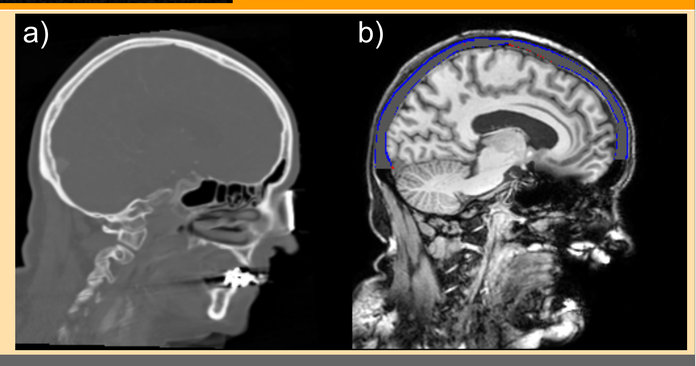

Fig. 4
Sagittal slices of a) the CT image, and b) the segmentation result overlaid onto T1-MRI. In b) false positive skull voxels are blue, and false positive ones are red.

IV CONCLUSION and OUTLOOK

We propose an automatic segmentation approach, which proves to be accurate especially with regard to the skull segmentation. From visual inspection and comparison to CT data we found that its accuracy is adequate for the construction of EEG head models. Our approach was implemented into an easy to use software pipeline (BESA MRI) allowing the effortless generation of individual, four-compartment realistic head models. Our development, thus, removes a substantial obstacle for the use of realistic head models in EEG source analysis.
To establish the accuracy of our approach we are currently performing another validation study with manual reference segmentations. Additionally, we are developing a tissue probability atlas to further increase the accuracy and robustness by incorporating additional a-priori knowledge on the anatomy of the human head.

[1] Yvert, B., Bertrand, O., Thévenet, M., Echallier, J. F., & Pernier, J. (1997). A systematic evaluation of the spherical model accuracy in EEG dipole localization. Electroencephalography and Clinical Neurophysiology, 102(5), 452–459.
[2] Lanfer, B., Paul-Jordanov, I., Scherg, M., & Wolters, C. H. (2012). Influence of interior cerebrospinal fluid compartments on EEG source analysis. In Proceedings BMT 2012 (Vol. 57). Presented at the 46. DGBMT Jahrestagung, Jena: De Gruyter.
[3] Dempster, A. P., Laird, N. M., & Rubin, D. B. (1977). Maximum Likelihood from Incomplete Data via the EM Algorithm. Journal of the Royal Statistical Society. Series B (Methodological), 39(1), 1–38.
[4] Lanfer, B., Scherg, M., Dannhauer, M., Knösche, T. R., Burger, M., & Wolters, C. H. (2012). Influences of skull segmentation inaccuracies on EEG source analysis. NeuroImage, 62(1), 418–431.
[5] Besag, J. (1986). On the Statistical Analysis of Dirty Pictures. Journal of the Royal Statistical Society. Series B (Methodological), 48(3), 259–302.
[6] Wang, D., Shi, L., Chu, W. C. W., Cheng, J. C. Y., & Heng, P. A. (2009). Segmentation of human skull in MRI using statistical shape information from CT data. Journal of Magnetic Resonance Imaging: JMRI, 30(3), 490–498.
[7] Dogdas, B., Shattuck, D. W., & Leahy, R. M. (2005). Segmentation of skull and scalp in 3-D human MRI using mathematical morphology. Human Brain Mapping, 26(4), 273–285.

Acknowledgment
The authors would like to thank Dr. Harald Kugel (University of Münster) and Dr. Matthias Köchling (formerly University Hospital, Münster) for providing some of the data for our validation study.

Corresponding author:
Benjamin Lanfer (benjamin.lanfer@besa.de)
Gräfelfing, Germany